Visual Abstract

Notch sensitivity study in u-notched polymers built by Additive Manufacturing (AM)

Jorge Guillermo Díaz Rodríguez, Alberto David Pertuz Comas, Juan David Sandoval Herrera
Universidad Industrial de Santander. Escuela de ingeniería mecánica, Carrera 27, calle 9. Bucaramanga, Colombia
jgdiazro@correo.uis.edu.co, https://orcid.org/0000-0002-0479-4827
apertuzc@uis.edu.co, https://orcid.org/0000-0002-9130-6528
juan.sandoval3@correo.uis.edu.co

ABSTRACT. Onyx ® is a new material composed of Polyamide 6 reinforced with short carbon fiber, used in the novel additive manufacturing composites technique. This paper aims to presents the axial fatigue performance of this material with and without U-notches. The experimentally determined S-N fatigue curve was obtained under axial load with a load inversion ratio, R = 0.1, and compared to fatigue performance of U-notched samples ranging from 0.25 to 2 mm radius. In addition, the stress concentration factor was compared for static and alternative loading to obtain the notch sensitivity in terms of the U-notch radius, showing that there is indeed a difference in stress concentration between them. The advantage of the approach is that it permits using commonly used dimensioning methods for this AM material.

KEYWORDS. Notch sensitivity, Uniaxial fatigue, Additive manufacturing, polymers.

OPEN ACCESS

Citation: Rodriguez, J. G. D., Comas, A. D. P., Herrera, J. D. S., Notch sensitivity study in u-notched polymers built by Additive Manufacturing (AM), Frattura ed Integrità Strutturale, 66 (2023) 127-139.

Received: 26.05.2023
Accepted: 02.08.2023
Online first: 06.08.2023
Published: 01.10.2023

INTRODUCTION

Fatigue notch sensitivity is a key factor to consider when designing a component. Notch sensitivity can be described as the material´s susceptibility to crack initiation and propagation under variable loading at notches, scratches, and other defects where stress concentration is higher [3].

On the other hand, Additive Manufacturing (AM) is a group of technologies that produce functional parts building components layer by layer, allowing complex shapes and geometries that may not be possible to manufacture by another method [8]. However, AM has not reached maturity [3], so there is room for improvement. From these technologies, material extrusion, MEX-TRB/P/Onyx, according to ISO/ASTM 52900:2021 [12], uses a thermoplastic polymer, which is probably the most popular [20]. However, due to the melting, deposition, and solidification of the thermoplastic polymer matrix, MEX gives a particular mechanical behavior with characteristics to consider while projecting a component [4,7,13]. Moreover, a recent review [6] identified missing mechanical characterization in these polymers. So, a research project was launched to find the notch sensitivity of a thermoplastic polymer used in MEX so parts can be projected with commonly known design methods.

AM processes generate time and material savings because producing one-part costs the same as producing many [14]. For example, the MEX technology developed by Markforged [31] uses a thermoplastic polymer as the matrix for continuous

fiber-reinforced composites. Onyx, which is polyamide 6 (commonly known as Nylon) with embedded chopped carbon fiber, is one of the polymers used as a matrix. It goes through a heated circular nozzle and is bonded by thermal reaction recreating the part layer by layer. That subsequent deposition leaves gaps between passes, giving an anisotropy intrinsic to most AM technologies, and was identified in the early years of AM development by [24]. A schematic of such gaps is shown in Fig. 1a for the material deposited in the Z direction and a SEM photograph of the actual gaps [22].

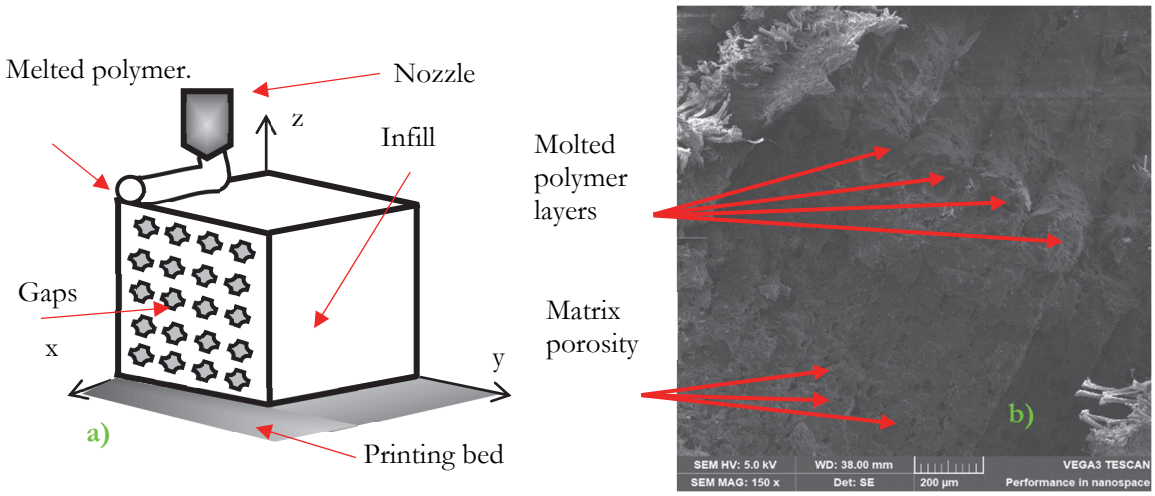

Figure 1: Porosity in MEX; a) schematics, b) actual porosity, adapted from [22].

Such gaps might behave as stress concentration sites on which the material may respond differently to static and alternative loads. The fatigue behavior of Nylon is complex and influenced by several factors, such as applied stress, notches, fiber content, and temperature [18]. A notch increases the stress field, see Fig. 2; the sharper the notch, the higher the stress gradient. Furthermore, a U-notch is a deeper than wider rounded-tip notch, whereas a V-notch end shows a null radius. U-notches show higher reproducibility than V-notches [15]. U-notches show higher reproducibility than V-notches [15]. Recently, Marsavina *et al.* [17] showed that, indeed V-notches require less energy than U-notches to fracture. Therefore, fatigue life decreases significantly with a reduced notch radius [11]. Hence, it is important to investigate the fatigue and fracture behavior of AM components in the presence of such notches [28].

There are different methods to predict the fatigue life of a notched component. For example, the method developed independently by Neuber (line method uses the average stress over a distance from r=0 to 2L) and Peterson (point method, uses r=L/2) to calculate the stress before the crack in the notch of the component, see Fig. 2a for the notation and Fig 2b for an example of an experimentally measured strain field where one can see how the strains go up radially as one gets closer to the notch. Another method, the theory of critical distances (TCD) developed by Taylor [30] considers as a material parameter the point where the fracture toughness, Kc, overcomes the strength of the material (σ_0) using Irwin´s plastic zone, see Eqn. (1).

$$L = \frac{1}{\pi}\left(\frac{Kc}{\sigma_0}\right)^2 \tag{1}$$

Although it was initially devised for metals, the TCD has given good agreements with experimental data for ceramics and brittle polymers such PPMA, PC or PS.

On the other hand, there are three fatigue methods components under variable stress: the stress-life (S-N) for components subjected over 1000 cycles, the strain-life (ε-N) method for components subjected up to 1000 cycles, and the da/dN method for cracked components. The notch sensitivity, *q*, is a parameter that tells the difference notch between static and alternating stress and is used in the S-N. The fatigue strength limit is generally measured by stress tests [3].

Fatigue tests for MEX polymers have been studied. In [7], a study was conducted on the fatigue resistance in notched polylactic polymer (PLA) samples printed by MEX. They used the critical distance theory (TCD). Pertuz *et al.* [21] studied the static and fatigue behavior of reinforced and non-reinforced Nylon printed by MEX in uniaxial tests, using the Weibull distribution to adjust the data obtained at each load level. Recently, Bandeira *et al.* [2] experimentally evaluated the flexural notch sensitivity of high-strength wires. First, they established tensile mechanical properties, and then they used the staircase method [3] to obtain the fatigue endurance limit for the notched and notched-free specimens. The difference in fatigue

performance between notched and notched-free specimens gives the notch sensitivity. Finally, Nijs *et al.* [19] used full-field strain measures to determine the notch sensitivity in a PP matrix carbon composite.

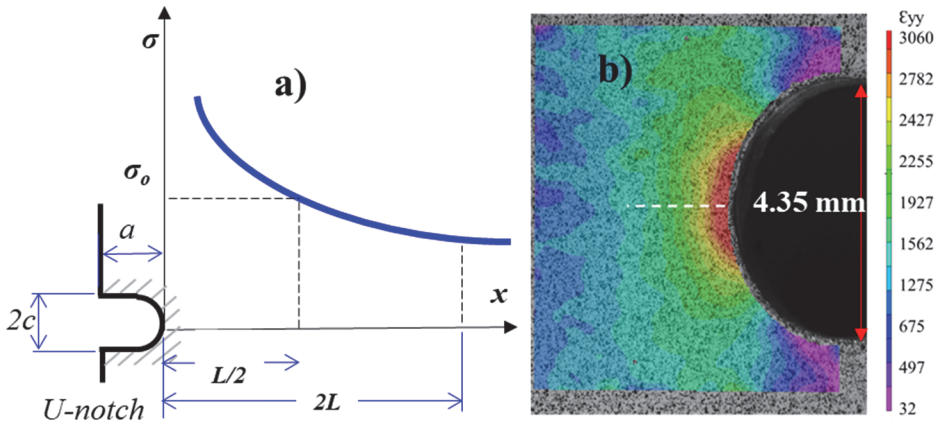

Figure 2: a) Stress distribution in front of a U-notch, b) Experimental strain in front of a round notch [5].

Several fatigue models have been used to predict the fatigue life of thermoplastic materials. For example, the Basquin model adjusts the data in uniaxial fatigue tests for notch and smooth samples [3].
To study smooth and notched Onyx ® fatigue behavior, Nylon based Polymer Matrix Composite (PMC) specimens used in AM were printed by MEX. Fatigue tests were performed under load reversal ratio R = 0.1. Five types of "U" notch with different radii were fatigue tested, and the data obtained by each were compared with uniaxial fatigue S-N from smooth specimens. Then, the difference in static and fatigue stress concentration is shown to extract the notch sensitivity. To the best of our knowledge, this is the first study on notch sensitivity for AM polymers reinforced with short carbon fiber. The paper shows the failure modes of the fatigue tests. This paper aims to find the notch sensitivity to use in accepted design methods.

THEORETICAL BACKGROUND

This section gives the baseline information for the reader to understand the paper.

Material extrusion

In 2015, Markforged [31] obtained a patent to manufacture MEX composites reinforced with continuous fibers. MEX is the most popular of AM. A schematic of the composite MEX printing process is shown in Fig. 3.

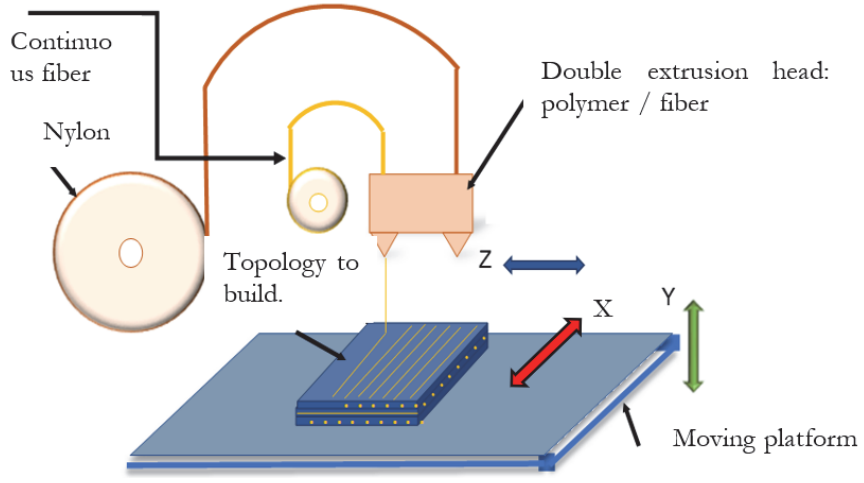

Figure 3: Schematics of composites MEX printing. Adapted from Ref. [14].

MEX is part of the AM family in which a slicer software layer reconstructs the geometry by layer from an STL file. For Markforged ®, this process is done by software in the cloud called Eiger® [31]. The mechanical properties for the matrix (Onyx ® and Nylon) are shown in Tab.1. First, it must be noted that Onyx ® is a composite itself, a nylon matrix reinforced with chopped carbon fiber.

Material	E [GPa]	σ [MPa]	Relative density	% Elongation
Nylon	1.7	33.5	1.1	4.5
Onyx	1.4	36	1.2	33
Standard	ASTM D638	ASTM D638	NA	ASTM D638

Table 1: Mechanical properties as provided by Markforged, [23].

Fatigue and stress concentration

When a discontinuity appears in a component and is subjected to fluctuating loads, it does not behave in the same way as a smooth component. This represents a change of cross section in the material, concentrating stress in the area where the notch is. The opening of a crack in a notch usually starts at the tip because that is where the maximum stress occurs, see Fig. 2. The stress concentration factor, K_t, was proposed by Inglis in 1913 for a plate with an elliptical hole under uniaxial load, and it can be estimated with Eqn. (2) with the notation depicted in Fig. 1. K_t depends only on the geometry and the load; therefore, it is a purely mechanical parameter.

$$K_t = 1 + 2\frac{a}{c} \tag{2}$$

The analysis of geometric and applied load to determine K_t is a complex problem, and one may not find a solution for a particular combination. Instead, it is determined by experimental techniques such as those compiled by Peterson, using an Airy stress function numerically or a combination of said methods [5]. In the case of an experimental approach, K_t can be calculated experimentally using Eqn. (3) [3].

$$K_t = \frac{\sigma_L}{\sigma_\infty} \tag{3}$$

where σ_L is the local stress at the notch and σ_∞ is the remotely applied static stress. However, if the remotely applied stress is alternative, the material might not behave the same. Therefore, the fatigue stress concentration factor, K_f, is used instead. The notch sensitivity, q shown in Eqn. (4), is a factor that tells the difference in stress concentrators due primarily to the geometry of the notch, the type of load, and the material. In this case, we also investigated if it is affected by the manufacturing method. The notch sensitivity for isotropic materials, such as metals, and selected polymers, can be found in the literature [3].

$$q = \frac{K_f - 1}{K_t - 1} \tag{4}$$

On the other hand, several fatigue models have been used to predict the S-N behavior of thermoplastic materials. The Basquin model is probably the most known, as seen in Eqn. (6).

$$\sigma = A\left(Nf\right)^b \tag{5}$$

where A and b are material constants that are determined experimentally. Furthermore, the Walker model introduces the effect of load ratio, R, as seen in Eqn. (6).

$$\sigma_{eq} = \sigma_a \left(\frac{2}{1-R}\right)^\gamma \tag{6}$$

where γ represents sensitivity to the load ratio, R, ranging between 0 and 1; for γ =0, the material is not sensitive, and for γ =1 is the most influenced by R. Furthermore, Ezeh and Susmel [7] recommended rules for estimating the S-N curve under different load ratios from static tests. Lu [16] tested several polymers with different stress ratios under alternative loads.

MATERIALS AND METHODS

The experimental procedure was divided into sample printing, static characterization, smooth and notched fatigue testing, and comparison of results.

The samples were manufactured with the MEX technique using the Mark Two printer [31] using ONYX which is Nylon embedded with short carbon fiber. Five smooth and 14 U-notched samples with 3 mm thickness were printed with the geometry shown in Fig. 4. The specimen geometry and notch radius values were determined according to the literature [2,7,10]. Finally, anisotropy is a well-documented effect for AM polymers [25] and AM in general [8]. Samples were printed following parameters from previous results [9], which included a solid matrix, and matrix deposition angle parallel to the load.

Tensile tests were performed within ASTM D639 guidelines on smooth samples at a 5 mm/min strain rate under displacement control. In addition, both static and fatigue tests were performed under displacement control using Eqn. (7).

$$d = \frac{PL}{AE} \tag{7}$$

where d is displacement, L is the initial calibrated length, A is the transversal area, E is elastic modulus, and P is applied load.

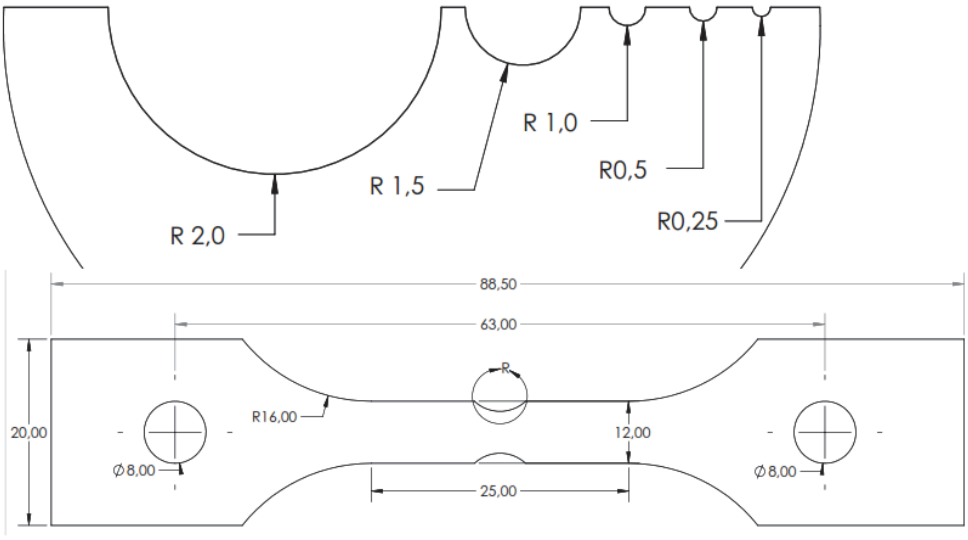

Figure 4: Samples geometry and measurements in (mm) of specimens.

Both static and fatigue tests used an MTS Bionix 370.02 equipped with a 25 kN load cell and an MTS 634.12F-25 extensometer measured axial deformation. Finally, fatigue tests were performed under controlled displacement using the linear elastic relation described in Eqn. (8).

The mechanical properties of ONYX thermoplastic were determined in tests under static load. Smooth samples were tested at constant amplitude at a 5Hz rate to estimate the S-N curve. After the curve was established, a nominal stress was applied in each notched sample to produce a local stress that made the sample last about 5000 cycles. The notched specimen's description is shown in Tab. 2. K_t values were calculated according to Peterson´s estimations [3].

A fractographic evaluation was performed to analyze the failure surface as well as the failure mechanisms under tensile and fatigue loading. First, samples were plated with gold and placed into a Vega 3 Tescan SEM between 7 and 10 keV equipped with a tungsten filament. However, after the gold plating was done in some samples, it made no difference for the SEM. This may be attributed to the chopped carbon fiber in the PA6 matrix that made the sample conductive.

Notch radius [mm]	Sample number	Quantity	K_t
0.25	1	2	2.92
0.5	2	3	2.78
1	3	3	2.52
1.5	4	3	2.27
2	5	3	2.03

Table 2: Notched specimens.

RESULTS AND DISCUSSION

The results of the tests and a first analysis are shown in this section.

Tensile tests

The tensile tests were performed for a solid configuration and Elastic modulus and strength were calculated. Fig. 5 shows the Stress vs. Strain curve; the material's ultimate stress (σ_{ut}) is approximately 45.8 MPa, and the Elastic modulus is 1094 MPa, with 99.94% of data represented by that value. [1] reported similar results, whereas [29] reported slightly lower values for PA6.

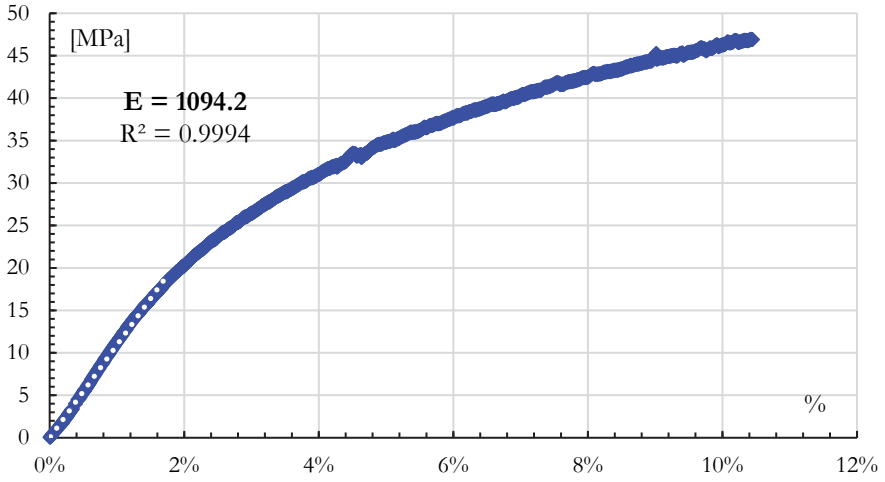

Figure 5: Static stress vs strain for Onyx

Fatigue tests on notched Onyx

The applied load P was determined by a percentage of the σ_{ut} to each sample for the fatigue tests. It is documented that polymers are time-dependent materials [4] they soften under variable loads [18]. According to a literature search [22,26] failure in polymer under fatigue loading can be described when the load fails below 85% of the initial load. The stress–life curve is shown in Fig. 6 for the stress produced when the applied load fell at 85% of the initial load. Furthermore, the data was adjusted to Basquin´s model rendering Eqn. (8), with 93.3% of the data represented by the constants. As a comparison, fatigue results [21] for MEX printed Nylon were added to Fig. 6 for different infill patterns (hexagonal with 50% density, triangular with 20 and 50% density). The results are very different below 100000 cycles, whereas for lives after 100000 cycles, the infill pattern seems to make no sizeable effect. Furthermore, the literature data reported and plotted in Fig. 6 is for Nylon, which is Onyx without the short carbon reinforcement.

$$\sigma = 2231.2\left(N_f\right)^{-0.514} \tag{8}$$

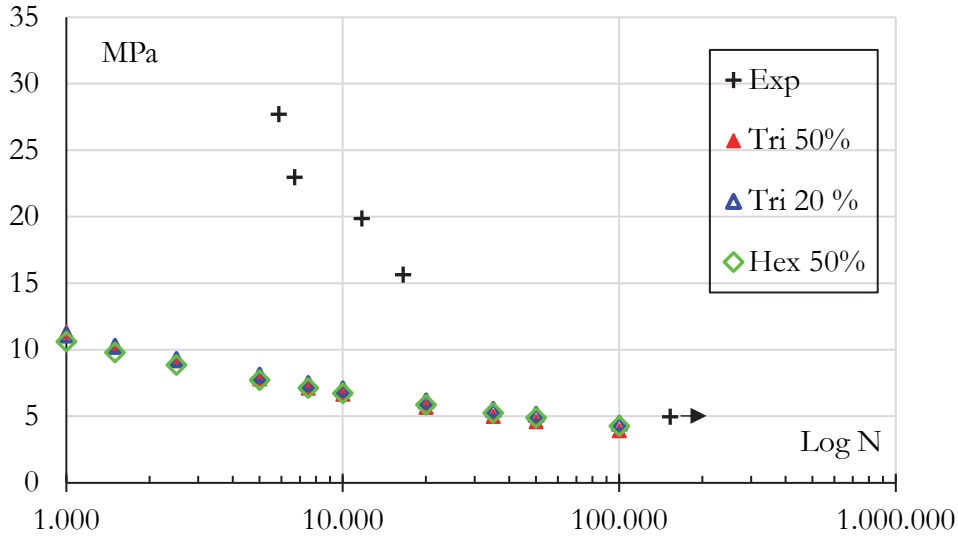

Figure 6: Experimental stress - life curve with comparison from [21].

It was also found how the thickness of the specimen changed over axial load, as depicted in Fig. 7, where the thickness went almost uniformly from 3 mm to about 1.95 mm after 1.18 million cycles.

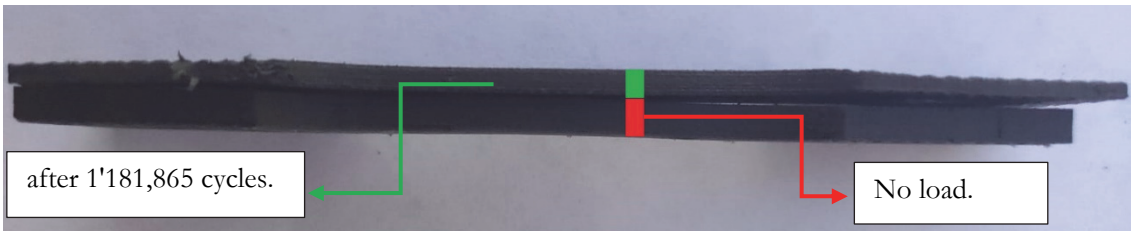

Figure 7: Exemplary results of change in thickness after 1181865 cycles.

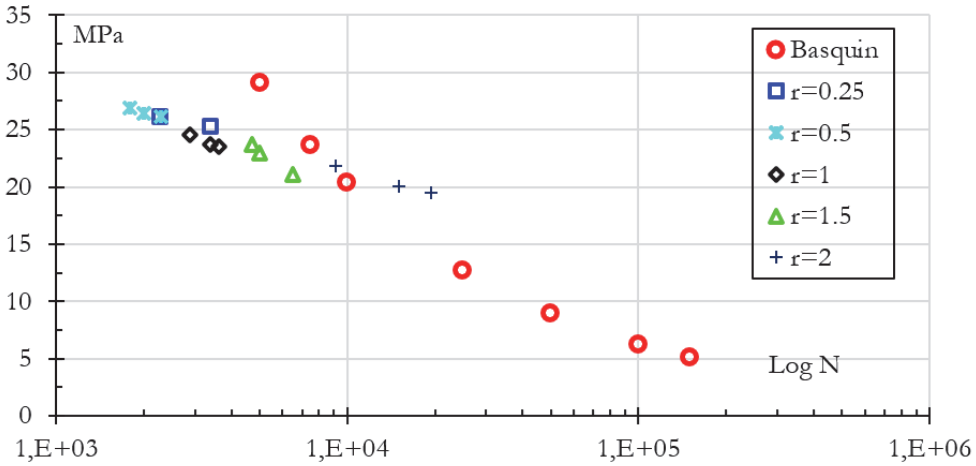

Figure 8: Stress - life curve for each notch sample.

Fatigue tests on notched Onyx

The "U" notch specimen description for each radius is shown in Tab. 2. When a specimen presented irregularities along the cross-section, it produced a stress concentration; therefore, such samples were rejected for testing. Moreover, with the Basquin constants, Eqn. (8), it was calculated the displacement, Eqn. (7), that caused a life of 5000 cycles for each notch with a stress concentration factor, Eqn. (3). The reference of 5000 cycles gave a nominal stress of 13.5 MPa. The S-N curve

is constructed for each notch configuration shown in Fig. 8. For the larger notch, the S-N curve overlaps with the notchless sample.
On the other hand, the smaller the radii are, the lower the specimen´s life. However, if the AM printed material had no notch sensitivity, the line would fall directly under the results for the larger notch. In this case, when the radii change, both the stress and life change simultaneously, meaning the material has notch sensitivity.
It was observed throughout the test that the crack starts at the notch´s corner, as shown in [7]. Fig. 9 shows how the crack began; Fig. 9a is at a side view, whereas Fig. 9b shows the front view. As time passed, the crack grew to run along the entire side of the notch, as shown in Fig. 9c. Notably, the crack initially grew on only one side of the notch, as shown in Fig. 9b.

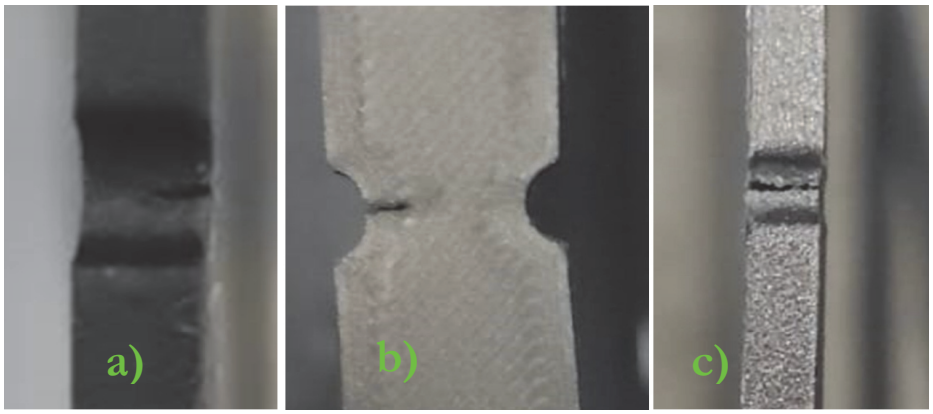

Figure 9: Crack growth in a U-notch for an initial 3 mm thick sample; a) lateral view of corner crack, b) front view of corner crack, c) through crack.

The presence of a notch considerably increases the stress in the vicinity of the discontinuity of the material. If a material behaves differently to the stress concentration under an alternative load, this is called notch sensitivity. This sensitivity depends on the material's mechanical properties as well as the type and stress on the notch. Therefore, one may estimate a stress concentration factor under an alternative load using Eqn. (9).

$$K_f = \frac{\sigma_{\text{notch}}}{\sigma_{\text{smooth}}} \tag{9}$$

So, the K_f value for each notch was estimated by comparing the average fatigue stress for U-notch samples with the Basquin stress at about 5000 cycles, as shown in Tab. 3. The value of K_f is always less than or equal to K_t [3]. So, the notch sensitivity q was estimated using Eqn. (4). The notch sensitivity is between 0 and 1. If q = 0, the material has no sensitivity to the notch, and K_f is equal to 1. On the other hand, if q = 1, the material has full notch sensitivity, and K_f is equal to K_t. When the notch sensitivity parameter is not known, the value of K_t is K_f or q=1 [3]. Tab. 3 shows the notch sensitivity for each configuration.

"U" sample	U notch radius, mm	σ smooth [MPa]	Average σ U-notch [MPa]	K_t	K_f	q
1	0.25	27.4	28.6	2.92	1.04	0.02
2	0.5	26.7	29.1	2.78	1.09	0.05
3	1	23.9	28.7	2.52	1.20	0.13
4	1.5	23.1	30.7	2.27	1.33	0.26
5	2.0	20.3	30.5	2.03	1.50	0.49

Table 3: Fatigue stress concentration factor, K_f.

Looking at the results in Tab. 3, one sees greater notch sensitivity for the larger notches. Fig. 10 shows the relationship between K_f, K_t, and q with notch radius. If there was no notch sensitivity, the relation between K_t and K_f should be parallel. The notch with a larger notch sensitivity value was the smallest notch radius because the fatigue concentration factor

increased. The sample with the sharpest notch had a higher stress concentrator and the lowest lower notch sensitivity. If q = 1 the material fully sensible to the notch and K_f is equal to K_t.

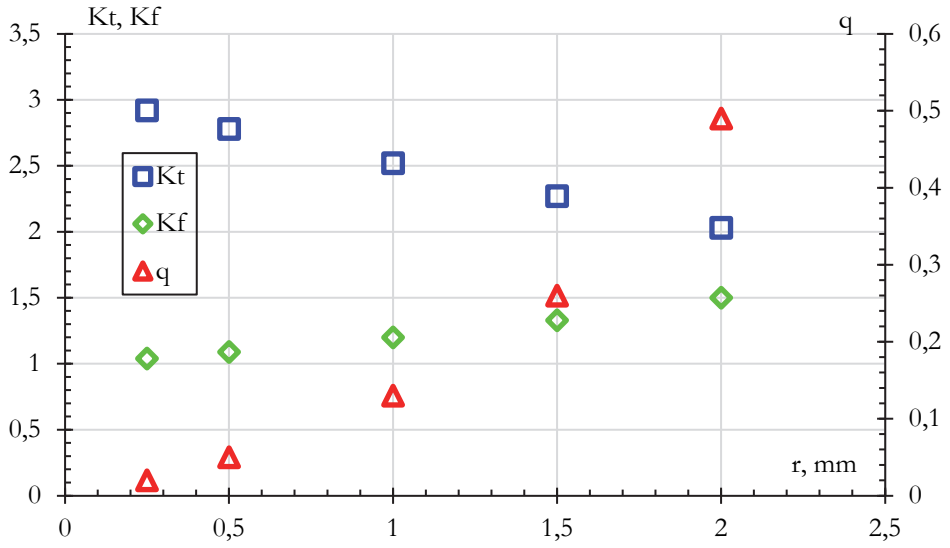

Figure 10: Stress concentration and notch sensitivity vs notch radius.

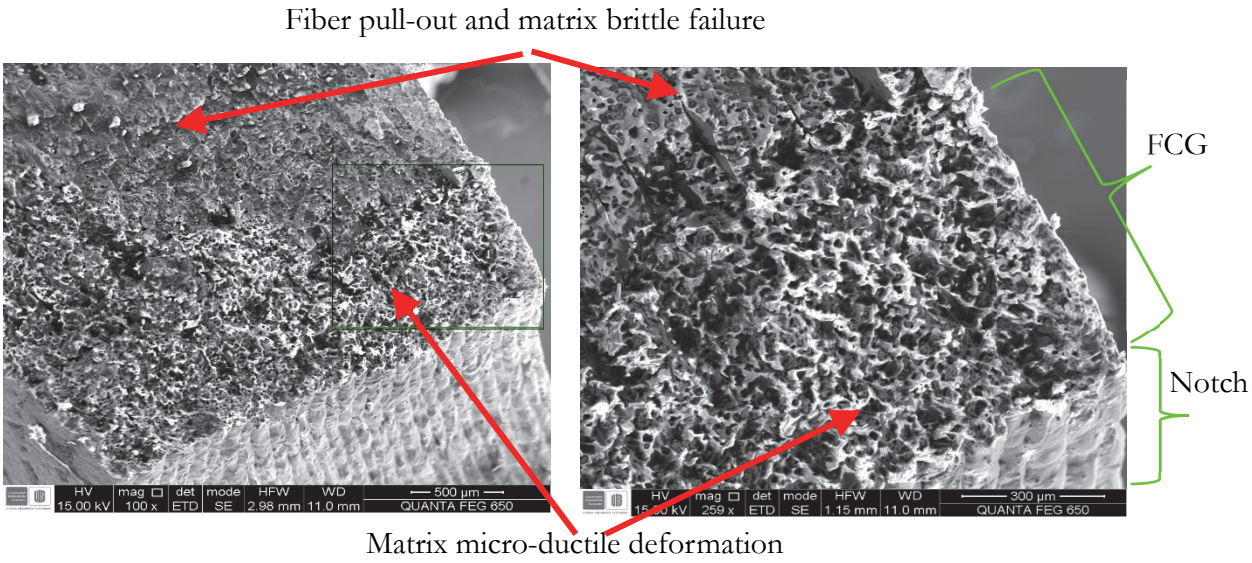

Figure 11: SEM image for the notched specimen with 2 mm radius.

Fractographic analysis

Polymers under cyclic load show a loss in elastic modulus [27]. Therefore, it was considered that the specimen had already failed when the load fell to 85% of the initial load [26]. Whether there was a crack or not, the sample had accumulated damage, so samples were broken under liquid nitrogen to reveal the failure surface. It is observed in Fig. 11 the fracture surface for a specimen with a notch radius of 2 mm is an area of many interstices observing the separation of the matrix from the short fibers, passing the nucleation process, helping the crack growth, and reaching the fracture of the specimen. One also sees parallel lines formed by the circular nozzle extruding molten polymer during the solidification process. Crazing is formed by the unraveling of polymeric chains, which macroscopically is perceived as a whitened area [4]. The alternative loading either causes a progressive rupture of fibrils at the point of the highest stresses or separation of the polymer matrix and fiber, thus becoming a crack. This rupture of fibrils is seen as a matrix micro-ductile failure. Finally, fatigue crack growth locations exposed fiber pull-out and matrix brittle failure, while crack initiation areas in the corners of fracture surfaces exhibited matrix micro-ductile deformation as reported in [18].

In Fig. 12, one can see how the shot carbon fiber sticks out of the nylon matrix and, simultaneously, the void spaces left by missing chopped fiber. Porosity is formed by the unfilled spaces left by the circular nozzle when the polymer is extruded. This porosity may be responsible for the material to exhibit lower strength and stiffness than a subtractive fabrication process. Although under cyclic loading the strain is redistributed by rearrangement of the polymer molecules at the microscopic level [18], polymers exhibit cyclic softening [21]. In Fig. 12, it can be seen that the nylon matrix and short carbon fibers are pulled out from each other, as reported in literature [18]. These are entirely broken due to the dynamic load applied. This is a drawback for AM materials because it causes fatigue resistance to be affected.

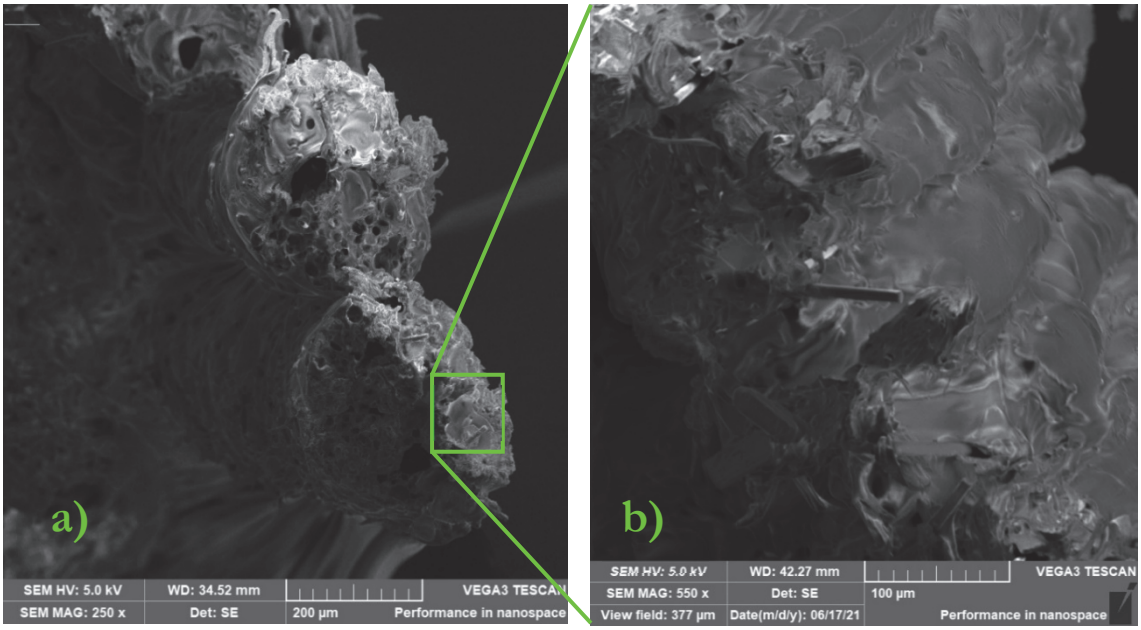

Figure 12: Molten layers showing short fiber pull-out.

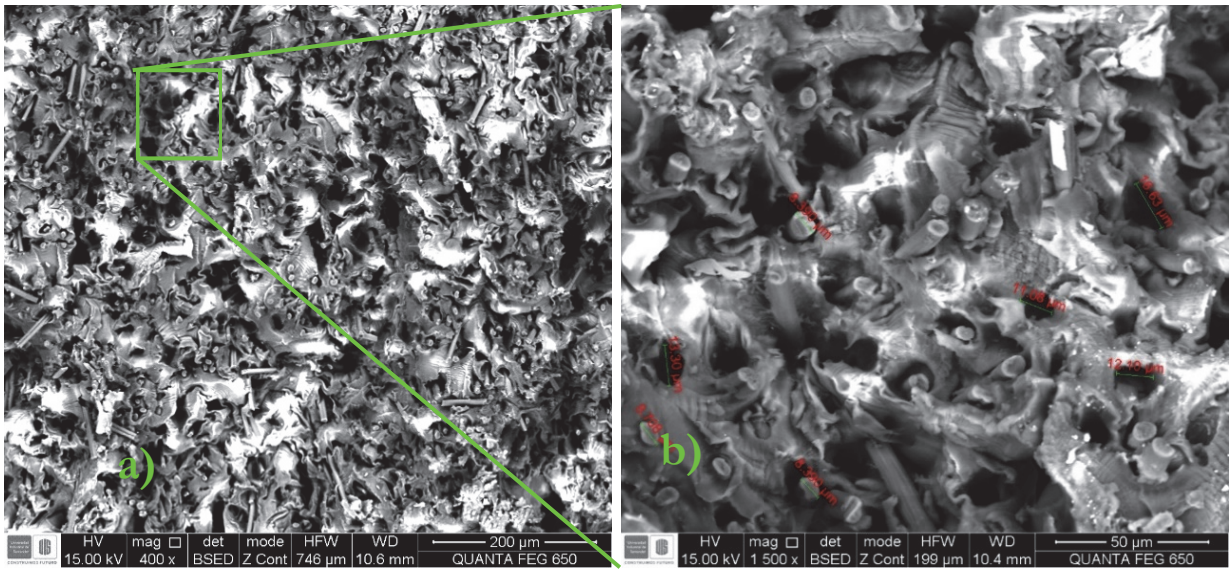

Figure 13: SEM image of the fracture zone for a specimen with a notch radius of 0.25 mm showing fiber breakage and fiber-matrix separation.

Fig. 13 shows that the nylon matrix looks deformed and somewhat crushed due to the forces it endured until it reached fracture. It also shows in more detail the short carbon fibers together with the nylon matrix. It shows the plastic deformation made by the fluctuating forces applied, as a material with a low plasticity can be considered fragile. The diameter of carbon fibers is approximately 8.4 microns [4]. Finally, it has to be said that a chopped fiber gets loose and under the SEM electric charge one can see it moving and get deformed while focusing the beam on it.

Finally, Fig. 14 shows different failure mechanics. The matrix layers that may leave porosity during solidification at different times; beach marks which were most likely produced by the alternating stress; and short fiber – voids which reveals how the material absorbed energy by pulling fiber out of the matrix. It is observed that porosity produced by adjacent matrix layers may act as a fatigue crack growth arrester. The growing crack finds a barrier in such discontinuities. This effect of crack arrest by printer layers was also noticed in [17], even for static loading.

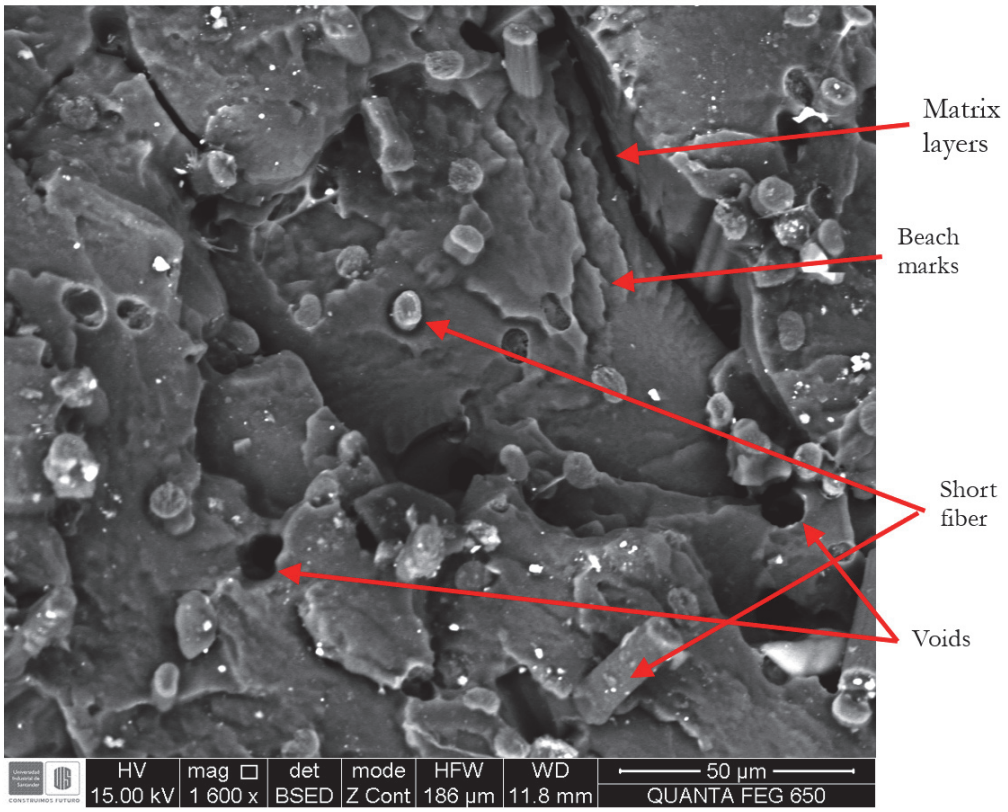

Figure 14: Close up of fracture surface in 1mm notch radius fatigued sample.

Conclusion

Static tests on a polymer matrix composite printed by material extrusion with solid configuration gave 45.8 MPa for ultimate stress and 1094 MPa for Elastic modulus. Furthermore, constant displacement tests produced stress-life data under a 0.1 load inversion ratio. Results were data fitted to the Basquin model rendering $\sigma = 2231.2N_f^{-0.514}$ for a smooth configuration. Finally, fractography revealed fatigue crack growth mechanisms, fiber pull-out, and matrix brittle failure.

It was seen the phenomena of load relaxation which has been documented for polymers. In this case, it was observed for a polymer matrix composite. The load relaxation began at an initial force and decreased as time passed until it remained constant for a long period. If one has a high K_t it will produce a greater stress riser; consequently, causing material failure. At the end of the tests, it was concluded that the number of cycles to fracture the Onyx material increased as the notch radius increased and vice versa.

The stress concentrator factor, K_f, made a difference for notched specimens under fatigue load. K_f roses as the notched radii grew. Notch sensitivity increases when the notch radius increases, but K_t decreases, and when K_t increases, notch sensitivity decreases as K_f. If this relationship between these variables did not occur, it would be very difficult to design parts capable of withstanding a nominal level of stress when they are in the presence of notches.

It is concluded that Onyx is a fatigue-resistant material when the notch radius increases due to the softness of the notch. On the other hand, with a small notch, the notch sensitivity decreases, and a high concentration of stresses produces the material's failure faster than a larger notch.

Acknowledgment

The authors acknowledge financial support from project VIE 2827, and the VIE mobility program at Universidad Industrial de Santander. The help of Tecnoparque SENA—Bucaramanga for printing some of the samples and to the center for electron microscopy at UIS is greatly appreciated.

References

[1] Ahmadifar, M., Benfriha, K., Shirinbayan, M. (2023). Thermal, Tensile and Fatigue Behaviors of the PA6, Short Carbon Fiber-Reinforced PA6, and Continuous Glass Fiber-Reinforced PA6 Materials in Fused Filament Fabrication (FFF), Polymers (Basel), 15(3), p. 507. DOI: 10.3390/polym15030507.

[2] Bandeira, C.F.C., Kenedi, P.P., Souza, L.F.G. de. (2017). Assessing the Notch Sensitivity of High Strength Wires, Latin American Journal of Solids and Structures, 14(13), pp. 2423–2438. DOI: 10.1590/1679-78253728.

[3] Castro, J.T.P., Meggiolaro, M.A. (2016). Fatigue Design Techniques, 3rd ed., USA, CreateSpace.

[4] Diaz, J.G., Pertúz, A.D., Ariza, C.J., García, D., Pinto, W. (2023). Monotonic crack propagation in a notched polymer matrix composite reinforced with continuous fiber and printed by material extrusion, Journal: Progress in Additive Manufacturing, 8(2). DOI: 10.1007/s40964-023-00423-w.

[5] Díaz-Rodríguez, J.G. (2022). Comparison of stress separation procedures. experiments versus theoretical formulation, Engineering Solid Mechanics, 10(2), pp. 153–164. DOI: 10.5267/j.esm.2022.1.003.

[6] Díaz-Rodríguez, J.G., Pertúz-Comas, A.D., González-Estrada, O.A. (2021). Mechanical properties for long fibre reinforced fused deposition manufactured composites, Compos B Eng, 211(January), p. 108657. DOI: 10.1016/j.compositesb.2021.108657.

[7] Ezeh, O.H., Susmel, L. (2020). On the notch fatigue strength of additively manufactured polylactide (PLA), Int J Fatigue, 136. DOI: 10.1016/j.ijfatigue.2020.105583.

[8] Gibson, I., Rosen, D., Stucker, B. (2015). Additive Manufacturing Technologies, New York, NY, Springer New York, DOI: 10.1007/978-1-4939-2113-3.

[9] González-Estrada, O.A., Pertuz Comas, A.D., Díaz Rodríguez, J.G. (2020). Monotonic load datasets for additively manufactured thermoplastic reinforced composites, Data Brief, 29, p. 105295. DOI: 10.1016/j.dib.2020.105295.

[10] Hu, X.A., Yang, X.G., Wang, J.K., Shi, D.Q., Huang, J. (2013). A simple method to analyse the notch sensitivity of specimens in fatigue tests, Fatigue Fract Eng Mater Struct, 36(10), pp. 1009–1016. DOI: 10.1111/ffe.12053.

[11] Ibáñez-Gutiérrez, F.T., Cicero, S., Carrascal, I.A. (2019). On the influence of moisture content on the fracture behaviour of notched short glass fibre reinforced polyamide 6, Compos B Eng, 159, pp. 62–71. DOI: 10.1016/j.compositesb.2018.09.062.

[12] ISO. (2021). ISO/ASTM 52900:2021. Additive manufacturing — General principles — Fundamentals and vocabulary.

[13] Kizhakkinan, U., Rosen, D.W., Raghavan, N. (2022). Experimental investigation of fracture toughness of fused deposition modeling 3D-printed PLA parts, Mater Today Proc. DOI: 10.1016/j.matpr.2022.10.014.

[14] León B., J., Díaz-Rodríguez, J.G., González-Estrada, O.A. (2020). Daño en partes de manufactura aditiva reforzadas por fibras continuas, Revista UIS Ingenierías, 19(2), pp. 161–175. DOI: 10.18273/revuin.v19n2-2020018.

[15] Liu, M., Gan, Y., Hanaor, D.A.H., Liu, B., Chen, C. (2015). An improved semi-analytical solution for stress at round-tip notches, Eng Fract Mech, 149, pp. 134–143. DOI: 10.1016/j.engfracmech.2015.10.004.

[16] Lu, Z., Feng, B., Loh, C. (2018). Fatigue Behaviour and Mean Stress Effect of Thermoplastic Polymers and Composites, Frattura Ed Integrità Strutturale, 12(46), pp. 150–157. DOI: 10.3221/IGF-ESIS.46.15.

[17] Marsavina, L., Negru, R., Serban, D., Marghitas, M., Popa, C. (2023). The notch effect on additive manufactured polymers, Procedia Structural Integrity, 47, pp. 744–748. DOI: 10.1016/j.prostr.2023.07.045.

[18] Mortazavian, S., Fatemi, A. (2015). Fatigue behavior and modeling of short fiber reinforced polymer composites including anisotropy and temperature effects, Int J Fatigue, 77, pp. 12–27. DOI: 10.1016/j.ijfatigue.2015.02.020.

[19] Nijs, A., Selezneva, M., Swolfs, Y., Hirano, N., Taketa, I., Karaki, T., Verpoest, I., Gorbatikh, L. (2020). Notch-sensitivity of hybrid carbon-fibre/self-reinforced polypropylene composites, Compos Sci Technol, 200, p. 108422. DOI: 10.1016/j.compscitech.2020.108422.

[20] Parrado-Agudelo, J.Z., Narváez-Tovar, C. (2019). Mechanical characterization of polylactic acid, polycaprolactone and Lay-Fomm 40 parts manufactured by fused deposition modeling, as a function of the printing parameters, ITECKNE, 16(2), pp. 25–31. DOI: 10.15332/iteckne.v16i2.2354.

[21] Pertuz, A.D., Díaz-Cardona, S., González-Estrada, O.A. (2020). Static and fatigue behaviour of continuous fibre reinforced thermoplastic composites manufactured by fused deposition modelling technique, Int J Fatigue, 130, p. 105275. DOI: 10.1016/j.ijfatigue.2019.105275.
[22] Pertuz-Comas, A.D., Díaz, J.G., Meneses-Duran, O.J., Niño-Álvarez, N.Y., León-Becerra, J. (2022). Flexural Fatigue in a Polymer Matrix Composite Material Reinforced with Continuous Kevlar Fibers Fabricated by Additive Manufacturing, Polymers (Basel), 14(17), p. 3586. DOI: 10.3390/polym14173586.
[23] REV 5.0 - 08/01/2021. (2021). Markforged composites mechanical properties. http://Static.Markforged.Com/Downloads/Composites-Data-Sheet.Pdf.
[24] Rodriguez, J.F., Thomas, J.P., Renaud, J.E. (2000). Characterization of the mesostructure of fused-deposition acrylonitrile-butadiene-styrene materials, Rapid Prototyp J, 6(3), pp. 175–186. DOI: 10.1108/13552540010337056.
[25] Rodríguez, J.F., Thomas, J.P., Renaud, J.E. (2003). Mechanical behavior of acrylonitrile butadiene styrene fused deposition materials modeling, Rapid Prototyp J, 9(4), pp. 219–230. DOI: 10.1108/13552540310489604.
[26] Saleh, M.A., Al Haron, M.H., Saleh, A.A., Farag, M. (2017). Fatigue behavior and life prediction of biodegradable composites of starch reinforced with date palm fibers, Int J Fatigue, 103, pp. 216–222. DOI: 10.1016/j.ijfatigue.2017.06.005.
[27] Shah, D.U. (2016). Damage in biocomposites: Stiffness evolution of aligned plant fibre composites during monotonic and cyclic fatigue loading, Compos Part A Appl Sci Manuf, 83, pp. 160–168. DOI: 10.1016/j.compositesa.2015.09.008.
[28] Shahbaz, S., Ayatollahi, M.R., Petru, M., Torabi, A.R. (2022). U-notch fracture in additively manufactured ABS specimens under symmetric three-point bending, Theoretical and Applied Fracture Mechanics, 119, p. 103318. DOI: 10.1016/j.tafmec.2022.103318.
[29] Stoia, D.I., Marsavina, L., Linul, E. (2021). Mode I critical energy release rate of additively manufactured polyamide samples, Theoretical and Applied Fracture Mechanics, 114, p. 102968. DOI: 10.1016/j.tafmec.2021.102968.
[30] Taylor, D. (2008). The theory of critical distances, Eng Fract Mech, 75(7), pp. 1696–1705. DOI: 10.1016/j.engfracmech.2007.04.007.
[31] Thomas, G., Antoni, M., Gozdz, S. (2015). Three dimensional printer with composite filament fabrication, USA patent US9156205B2.